

The Extreme Scattering Event Toward 1741–038: H I Absorption

T. Joseph W. Lazio

Naval Research Laboratory, Code 7213, Washington, DC 20375-5351, USA

lazio@rsd.nrl.navy.mil

R. A. Gaume

US Naval Observatory, 3450 Massachusetts Ave. NW, Washington, DC 20392-5420, USA

rgaume@usno.navy.mil

M. J. Claussen

National Radio Astronomy Observatory, P. O. Box O, Socorro, NM 87801, USA

mclausse@nrao.edu

A. L. Fey

US Naval Observatory, 3450 Massachusetts Ave. NW, Washington, DC 20392-5420, USA

afey@usno.navy.mil

R. L. Fiedler

Naval Research Laboratory, Code 7261, Washington, DC 20375-5351, USA

fielder@sealab.nrl.navy.mil

and

K. J. Johnston

US Naval Observatory, 3450 Massachusetts Avenue NW, Washington, DC 20392, USA

kjj@astro.usno.navy.mil

ABSTRACT

We report multi-epoch VLA H I absorption observations of the source 1741–038 (OT–068) before and during an extreme scattering event (ESE). Observations at four epochs, three during the ESE, were obtained. We find no changes in the equivalent width, maximum optical depth, or velocity of maximum optical depth during the ESE, but we do find a secular trend of decreasing maximum optical depth between our observations and ones by other observers a decade prior. The resulting limit on the H I column density change during the ESE for a structure with a spin temperature T_s is $6.4 \times 10^{17} \text{ cm}^{-2} (T_s/10 \text{ K})$. Tiny-scale atomic structures (TSAS), with $N_H \sim 3 \times 10^{18} \text{ cm}^{-2}$, are ruled out marginally by this limit, though geometric arguments may allow this limit to be relaxed. Galactic halo molecular clouds, that are opaque in the H I line, cannot be excluded from causing the ESE because the observed velocity range covers only 25% of their allowed velocity range.

Subject headings: ISM: structure — quasars: individual (1741–038) — radio lines: ISM

1. Introduction

Extreme scattering events (ESE) are a class of dramatic changes in the flux density of radio sources (Fielder et al. 1994). They are typically marked by a decrease ($\gtrsim 50\%$) in the flux density near 1 GHz for a period of several weeks to months, bracketed by substantial increases, viz. Figure 1. Because of the simultaneity of the events at different wavelengths, the time scales of the events, and light travel time arguments, ESEs are likely due to strong scattering by ionized structures, possibly in the Galactic interstellar medium (ISM; Fiedler et al. 1987a; Romani, Blandford, & Cordes 1987; Walker & Wardle 1998). First identified in the light curves of extragalactic sources, ESEs have since been observed during a timing program of the pulsars PSR B1937+21 (Cognard et al. 1993; Lestrade, Rickett, & Cognard 1998) and PSR J1643–1224 (Maitia, Lestrade, & Cognard 1998).

Modelling of ESE light curves leads to inferred densities $n_e \gtrsim 10^2 \text{ cm}^{-3}$ within these ionized structures (Romani et al. 1987; Clegg, Fey, & Lazio 1998). In turn, these densities imply pressures $nT \sim 10^6 \text{ K cm}^{-3}$ or more, well in excess of the “average” interstellar pressure $nT \sim 3000 \text{ K cm}^{-3}$ (Kulkarni & Heiles 1988).

A key issue regarding these ionized structures is their relationship to other phases of the interstellar medium. Do they represent (relatively) isolated structures, perhaps in pressure balance with a lower density, higher temperature “background” phase (Clegg, Chernoff, & Cordes 1988)? or do they reflect a low level of cosmic-ray ionization within an otherwise neutral structure (Heiles 1997)? or are they perhaps not interstellar at all, but due to photoionized molecular clouds in the Galactic halo (Walker & Wardle 1998)?

This paper reports the first H I absorption measurements of a source (1741–038, OT–068) while it was undergoing an ESE. From these observations we can constrain the connection between the ionized structures responsible for ESEs and any neutral structures. In §2 we describe the observations, in §3 we discuss the implications of our observations, and in §4 we present our conclusions and suggestions for future work.

2. Observations and Analysis

Figure 1 shows a portion of the 2.25 and 8.3 GHz light curve of 1741–038 as obtained by the US Navy’s extragalactic source monitoring program at the Green Bank Interferometer (Fiedler et al. 1987b; Lazio et al. 2000a). Clearly evident is an approximately 50% decrease in the source’s flux density at 2.25 GHz and an approximately 25% decrease at 8.3 GHz. The minimum occurred on or near 1992 May 25 (JD 2448768.264), and the 2.25 GHz flux density of the ESE is nearly symmetric about this epoch. The complete GBI light curve of 1741–038, extending from 1983 to 1994, has been published previously (Clegg et al. 1998).

We used the VLA to measure the H I absorption toward 1741–038 at four epochs. Figure 2 shows these four epochs; Table 1 summarizes the observing logs for the four epochs. The first epoch, 1991 September 6, was prior to the onset of the ESE and shall be used as a control. The remaining three epochs occurred during the ESE. During the first epoch, full circular polarization was recorded; only right circular polarization was recorded for the three epochs during the ESE. At all four epochs on-line Doppler corrections and on-line Hanning smoothing were applied. A bandwidth of 0.78 MHz was recorded in 256 channels, producing a velocity resolution of 0.64 km s^{-1} . The observations on 1992 June 6 also included a comparable amount of observing time with an observing bandwidth of 1.56 MHz in 256 channels, producing a velocity resolution of 1.29 km s^{-1} . We calibrated these data following the same procedures described below for the narrower bandwidth observations. As these wider bandwidth observations were obtained at only a single epoch, we will focus largely on the narrower bandwidth observations. We will use the wider bandwidth observations only to test for the possibility of H I absorption at large velocities.

For the three ESE epochs, observing runs consisted of scans on 3C 48 and 3C 286, for flux density calibration, and “on-line” and “off-line” scans of 1741–038. On-line scans were centered on an LSR velocity of 0 km s^{-1} and included the H I line. Off-line scans were centered at an LSR velocity of -360 km s^{-1} ; the scans on 3C 48 and 3C 286 were frequency-shifted by an amount

TABLE 1
VLA OBSERVING LOG

Epoch	VLA Configuration	Synthesized Beam (")	Polarization	Bandwidth (MHz)	Velocity Resolution (km s^{-1})	On-Source Time (hr)	Flux Density (Jy)
1991 September 6	A	2.5	R, L	0.78	0.64	0.66	2.13
1992 June 6 ^a	DnC	50	R	0.78	0.64	2.2	0.59
1992 June 6 ^a	DnC	50	R	1.56	1.29	2.2	0.59
1992 June 24	DnC	50	R	0.78	0.64	3.3	0.71
1992 July 28	D	50	R	0.78	0.64	3.5	1.92

^aObservations on 1992 June 6 were obtained quasi-simultaneously with both 0.78 and 1.56 MHz bandwidths.

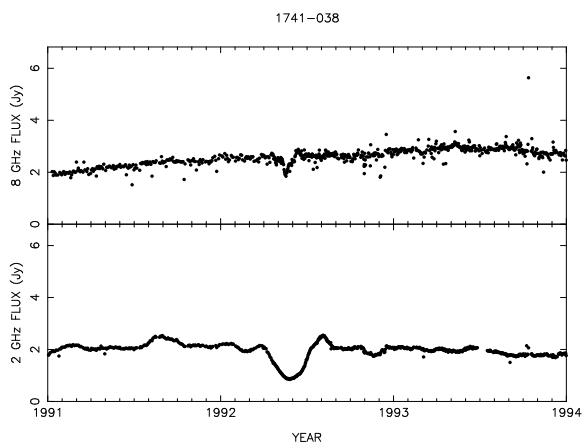


Fig. 1.— The extreme scattering event toward 1741–038. The upper panel shows the 8.3 GHz light curve, and the lower panel shows the 2.25 GHz light curve. Both light curves were obtained with the Green Bank Interferometer.

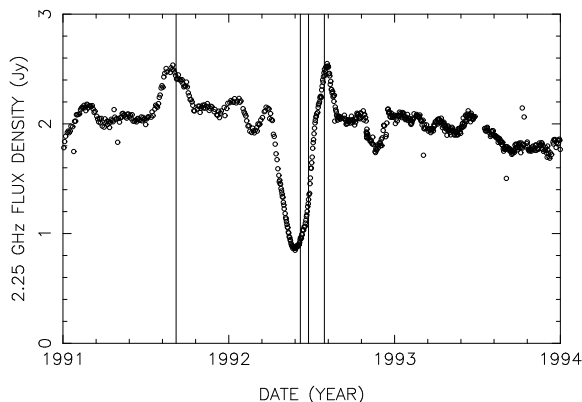


Fig. 2.— The epochs of H I absorption during the ESE of 1741–038. The dots show the 2.2 GHz flux densities measured by the Green Bank Interferometer. The vertical lines indicate the epochs at which H I absorption observations were acquired.

between -360 and -442 km s^{-1} . For the 1991 September 6 epoch, there were no off-line scans of 1741–038, the on-line scans of 1741–038 were centered at an LSR velocity of 30 km s^{-1} , only 3C 286 was observed for flux density calibration purposes, and the scans of 3C 286 were frequency shifted to -200 km s^{-1} and $+200 \text{ km s}^{-1}$.

Figure 3 shows the H I emission spectrum obtained by a single VLA antenna on 1992 June 24. The emission spectra from the other three epochs are similar; in particular, the spectra at the other two ESE epochs show no deviations above the 2σ level within the H I line. The shape of the line on 1991 September 6 is identical, though the maximum amplitude of the line differs by approximately 10%. We would not expect any change during the ESE because the large primary beam of the VLA antennas means that they are sensitive to H I emission on angular scales much larger than any structures plausibly responsible for the ESE itself. The emission spectra we obtain are in generally good agreement with that found by Dickey et al. (1983) using the NRAO 90 m telescope: The peak emission occurs near 5 km s^{-1} , and the emission is skewed toward positive velocities. The width of the emission line from our spectrum and the brightness temperature of the line are larger than that found by Dickey et al. (1983) owing to the smaller diameter antenna in our case (25 m vs. 90 m).

Because we are searching for changes in an absorption line with time, we discuss in detail the steps we took to calibrate these observations. Our primary focus will be on the three observations with a common bandwidth and velocity resolution during the ESE. The calibration of the wider

bandwidth observations on 1992 June 6 was identical to the procedure described below. The calibration of the first epoch, 1991 September 6, was extremely similar; we shall only point out the minor ways in which it differed from the calibration of the other four observations.

The conventional calibration of spectral-line observations involves determining a bandpass correction. With such widely distributed emission as for the H I line, position-switched observations of another source cannot be utilized to find the bandpass correction, and frequency switching requires observations both above and below the H I line. Furthermore, frequency switching can introduce phase jumps, which would then be propagated into the bandpass correction, and errors introduced in the frequency switching ultimately limit the bandpass that can be obtained (Wilcots, Brinks, & Higdon 1997). In this case, frequency-switched observations both above and below the H I line were available only on 1991 September 6 and then only for 3C 286.

More important than the shape of the bandpass during any particular observation, however, is its stability from one observation to the next, particularly during the ESE. In order to assess this stability, we constructed bandpass corrections for each of the three ESE epochs using the off-line scans on 1741–038. For any given antenna at any epoch, the amplitude of the bandpass correction was within 8.4% of unity with a standard deviation of approximately 5% and the maximum phase correction was no more than $7^{\circ}.5$ with a standard deviation of approximately 5° .

We decided ultimately to forego a bandpass correction. As further insurance against any bandpass-induced changes, we also excluded the first and last 16 channels from the analysis. We also repeated the calibration described here for the 1992 June 6 observations, including various bandpass calibrations determined from the off-line scans of 1741–038. We discuss the results in more quantitative detail below, but the lack of a bandpass calibration produces no significant change in the absorption spectra we measure.

Amplitude calibration was performed using 3C 48 and 3C 286. The frequency offsets between the on-line scans and the frequencies at which 3C 48 and 3C 286 were observed contribute to less than a 0.1% bias in the flux density cali-

bration. Far more important is the contribution of the H I line emission to the system temperature of the on-line scans. In order to avoid a bias, we determined the antenna gain amplitudes for 1741–038 using the off-line scans only, then applied these to both the on- and off-line scans. For the 1991 September 6 observations, for which no off-line scans of 1741–038 were available, we used channels well outside the range over which the H I emission was seen. Typical differences between the flux densities on- and off-line were 10–15%. As 1741–038 is itself a VLA calibrator and well approximated by a point source over the range of available baselines, the visibility phases were calibrated using the off-line scans on 1741–038 itself.

The observations during the three ESE epochs were acquired when the VLA was in its most compact configurations (DnC and D). In these configurations the H I emission may not be entirely resolved out, particularly on the shortest baselines. As a result there may be contamination of the H I spectra from the changing sky distribution of the H I emission moving through the VLA’s sidelobes as the VLA tracks the source (Goss, van Gorkom, & Shaver 1979). After amplitude and phase calibration, we inspected the visibility amplitudes and phases on the shorter baselines for evidence of H I line contamination. We found that some shorter baselines did show phase and/or amplitude offsets characteristic of such contamination. As a precaution we eliminated baselines shorter than 125 m (600λ) from further analysis for all epochs.

Before imaging the data, a single iteration of phase-only self-calibration was performed on a single continuum channel in the on-line data. The starting model was a point source, with the flux density appropriate for each epoch (Table 1). 1741–038 is well approximated by a point source for all VLA configurations, and we subtracted the continuum in the visibility domain, utilizing line-free channels of the on-line data to generate a linear baseline. We imaged and CLEANed each channel of the data cube separately. We also produced a continuum image from the line-free channels of the on-line data (prior to performing the continuum subtraction). Absorption spectra were formed by integrating the continuum-subtracted data cube over a region whose size was that of the synthesized beam and which was centered on the

position of 1741–038. These were converted to opacity spectra using the flux density determined by fitting a gaussian function to the continuum image.

Figure 4 shows the resulting H I opacity spectra for the four epochs. All of the spectra show the presence of a strong absorption feature near 5 km s^{-1} , a slight curvature resulting from the absence of a bandpass correction, and a typical rms determined outside the H I line of $\sigma_\tau \approx 0.012$. Our absorption spectra are in good agreement with that found by Dickey et al. (1983).

As a further assurance that our lack of a bandpass calibration has not introduced significant uncertainties, we repeated the above analysis using two different bandpass corrections applied to the 1992 June 6 observations. We applied a bandpass correction determined from the off-line scans of 1741–038 from 1992 June 6 and from 1992 June 24. In both cases, the spectral baseline after correction is more nearly constant with velocity. The rms uncertainty in the opacity spectrum increases slightly with the application of the 1992 June 6 bandpass correction and little, if at all, with the application of the 1992 June 24 bandpass correction. The increase in the rms uncertainty is approximately 25% from $\sigma_\tau \simeq 0.012$ to $\sigma_\tau \simeq 0.015$. In order to account for the uncertainties resulting from the lack of a bandpass calibration and from any possible changes between epochs, we shall use the value $\sigma_\tau = 0.015$ as the value for the typical uncertainty in the opacity spectrum at all three epochs during the ESE.

3. Discussion

In this section we first assess the extent to which there are any changes in the absorption spectra. We then discuss what this implies about neutral structures along the line of sight to 1741–038 during the ESE.

3.1. Line Changes

We shall consider three quantities that might be expected to change during the ESE—the equivalent width of the H I line, $W \equiv \int dv \tau(v)$; the maximum absorption and its velocity; and the shape of the line. Table 2 summarizes these observable quantities at the four epochs.

There is no gross change in the absorption line,

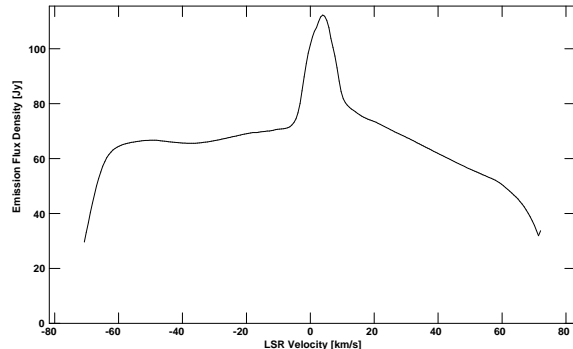


Fig. 3.— The H I emission spectrum as measured by a single VLA antenna on 1992 June 24. No bandpass calibration has been applied. Emission spectra from the other two epochs during the ESE are similar at the 2σ level.

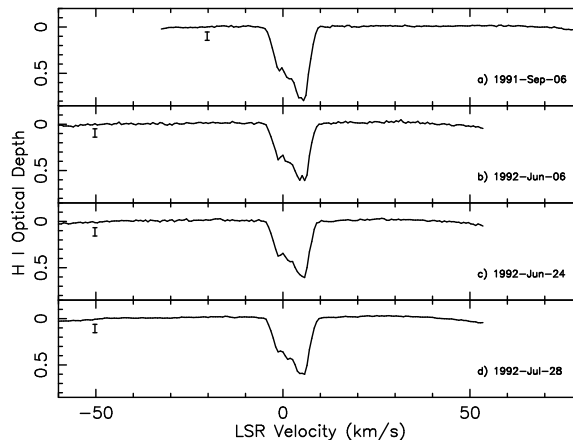


Fig. 4.— The H I opacity spectra toward 1741–038, see also Figure 2. All spectra were obtained by spatially integrating the brightness distribution of 1741–038 at every frequency channel over a region comparable to the half-power width of the synthesized CLEAN beam. Our angular resolution is such that 1741–038 is unresolved, so we do not show the images for these epochs. Shown in the upper left of each figure is the $\pm 3\sigma$ uncertainty in the optical depth, determined from a region of the spectrum where there is no absorption. (a) The epoch 1991 September 6, before the ESE. This observation was centered at an LSR velocity of 30 km s^{-1} , so the velocity range is different than for the other three epochs. (b) The epoch 1992 June 6. (c) The epoch 1992 June 24. (d) The epoch 1992 July 28.

TABLE 2
OBSERVABLE QUANTITIES AT EACH EPOCH

Epoch	τ_{\max}	v at τ_{\max} (km s ⁻¹)	W (km s ⁻¹)	$\max(\Delta\tau)$	Epoch of $\max(\Delta\tau)$
1991 September 6	0.79	5.5	6.27
1992 June 6	0.61	5.8	4.80	0.049	1992 June 24
1992 June 24	0.61	5.8	4.77	0.049	1992 June 6
1992 July 28	0.60	5.8	4.83	0.045	1992 June 6

NOTE.— τ_{\max} is the maximum optical depth. $\max(\Delta\tau)$ is the maximum difference in optical depths between two epochs. For a given epoch the maximum difference in optical depth occurs between itself and the epoch listed in Column 6.

particularly during the ESE. The maximum optical depth for the ESE epochs is $\tau \simeq 0.61$ and occurs at 5.8 km s⁻¹. The equivalent width is $W \approx 4.8$ km s⁻¹, and from Table 2 the maximum difference in W between any two epochs is 0.03 km s⁻¹. We estimate the uncertainty in W as $\sigma_W = \sigma_\tau \Delta v$ where Δv is the velocity extent of the line, $\Delta v \approx 10$ km s⁻¹. Thus, $\sigma_W \approx 0.15$ km s⁻¹, and we conclude that there has been no change in the equivalent width of the line.

One notable difference between the absorption spectra of 1991 September 6 and the ESE epochs is the change in the maximum optical depth. The maximum optical depth for all four of our epochs also differs from previous observations by Dickey et al. (1983), $\tau_{\max} \approx 1$, and Dickey & Benson (1982), $\tau_{\max} \approx 3$. Dickey & Benson (1982) observed 1741–038 using an interferometer composed of the NRAO 140 ft and 300 ft telescopes in 1980 and 1981. Dickey et al. (1983) observed 1741–038 using the phased VLA in 1982. There is some danger in comparing observations from different telescopes, and the large optical depth found by Dickey & Benson (1982) has a large uncertainty associated with it. Nonetheless, these changes in the optical depth are indicative of a decreasing secular trend in the H I column density by 50% or more over the decade between the various observations.

Qualitatively, there do appear to be fine scale changes in the line shape from epoch to epoch dur-

ing the ESE. In particular the line has two, nearly equally deep minima on 1992 June 6, but only a single deep minimum in the other two epochs. We assess the significance of this difference in the line shape quantitatively by finding the maximum difference in optical depth between two epochs at the same velocity (Columns 4 and 5 of Table 2).

The maximum optical depth difference between any two epochs occurs between 1992 June 6 and June 24 and is $\max(\Delta\tau) = 0.049$. The maximum difference between 1992 June 6 and July 28 is 0.045. (The difference between 1992 June 24 and July 28 is half this value, reflecting their qualitatively more similar shapes.) We do not regard any of these differences as significant. The rms uncertainty in an individual opacity spectrum is $\sigma_\tau = 0.015$. Adding the uncertainties from two spectra in quadrature, the combined uncertainty is 0.021, meaning that the maximum deviation is less than 2.3σ . We have also examined the difference spectra (i.e., the spectra formed by taking the difference in the absorption spectra at two epochs) for any skewness. If line features either appear or disappear, one would expect an excess of either positive or negative deviations about the average. Conversely, if the deviations are simply the result of measurement uncertainty, there should be a roughly equal number of positive and negative deviations about the average. The latter is the case for all three difference spectra.

In addition to the line shape not changing by

any significant amount, there is also no evidence for the appearance of additional absorption components at other velocities. The only significant absorption occurs between -5 and 10 km s^{-1} for all four epochs. We can also compare the absorption spectrum from our wider bandwidth (1.56 MHz ; 1992 June 6) to those of Dickey et al. (1983) as they have a similar velocity coverage. Both spectra have a single deep absorption feature, with no significant absorption outside of it.

3.2. ESE Structures

Our limit on changes in the optical depth during the ESE of $\Delta\tau < 0.05$ implies the neutral column density change during the ESE must be limited to

$$\Delta N_H < 6.4 \times 10^{18} \text{ cm}^{-2} \left(\frac{T_s}{100 \text{ K}} \right) \quad (1)$$

for the structure(s) responsible for the ESE. Here T_s is the spin temperature of the H I within the structure, and we have assumed that the structure responsible for this ESE is optically thin to H I radiation. This assumption is justified by the lack of a large change in the H I profile.

We consider $T_s \approx 200 \text{ K}$ and $T_s \sim 10 \text{ K}$ as possible values for T_s . The former value is motivated from observations by Dickey & Benson (1982) who find a typical value of $T_s \sim 200 \text{ K}$ for 14 lines of sight with a Galactic latitude $10^\circ < |b| < 20^\circ$ (1741–038 has $b = 13^\circ$ and is one of the 14 lines of sight observed). The latter value is motivated from models by Heiles (1997) and Walker & Wardle (1998), who have both proposed a population of cold, small-scale structures.

If $T_s \approx 200 \text{ K}$, then $\Delta N_H < 1.3 \times 10^{19} \text{ cm}^{-2}$. This is not a stringent limit. Models of ESE lenses require electron column densities $N_e \sim 10^{16} \text{ cm}^{-2}$ (Fielder et al. 1994; Clegg et al. 1998). We presume that any H I structure associated with an ESE lens will have a size scale of order the ESE lens, namely AU scale. If the neutral structure is in approximate pressure balance *with the ESE lens* (which itself may be overpressure with respect to the ambient medium, §1), then the neutral structure would have column densities $N_H \sim 10^{18} \text{ cm}^{-2}$, well below this observational limit.

If $T_s \sim 10 \text{ K}$, then $\Delta N_H < 6.4 \times 10^{17} \text{ cm}^{-2}$. This limit marginally rules out Heiles’ (1997) pro-

posed tiny-scale atomic structures (TSASs) as being responsible for the ESE. TSASs are AU-scale structures distributed throughout the Galactic interstellar medium with neutral column densities $N_H \sim 3 \times 10^{18} \text{ cm}^{-2}$ and interior temperatures $T_s \sim 15 \text{ K}$. Heiles (1997) proposes TSASs in order to explain observations of small (angular) scale changes in the H I opacity, though he does not associate TSASs explicitly with ESEs.

Obviously, geometrical factors (e.g., a line of sight that does not cut through the center of a TSAS) could account for the discrepancy. Other indications of an association between TSASs and ionized structures are also not clear-cut. In favor of an association is that Clegg et al. (1998) reproduced the ESE light curve of 1741–038 by assuming a gaussian refracting lens passed in front of the source; they find an electron column density of $10^{-4} \text{ cm}^{-3} \text{ pc}$ is required to produce the light curve, comparable to what the TSASs should have in their interiors due to photoionization (Heiles 1997). On the other hand a comparable change in the dispersion measure of PSR B0823+26 occurred (Phillips & Wolszczan 1991) with no change in the H I opacity (Frail et al. 1994). Though, after the conclusion of the DM monitoring program, an H I opacity change was detected.

Our limit on ΔN_H appears to rule out Galactic halo molecular clouds, the AU-scale, H I-opaque structures that Walker & Wardle (1998) have proposed to explain ESEs. The photoionized skins of these clouds would provide the necessary refracting media for ESEs. We see no indication of a $\tau > 1$ feature in our spectra (though Walker 2000, private communication, has since suggested that $\tau \sim 0.1$ might be more accurate). Walker & Wardle (1998) point out that, because of multiple imaging, an H I absorption line during an ESE could saturate with a non-zero intensity, but Lazio et al. (2000b) find no evidence of multiple imaging in VLBI images of 1741–038 acquired at similar epochs as these H I absorption measurements. However, as halo objects, the clouds could have velocities approaching 500 km s^{-1} (i.e., a velocity range of 1000 km s^{-1}). The velocity range of our observations, even the wide bandwidth observations of 1992 June 6, is considerably less, being no more than 250 km s^{-1} . Thus, a significant H I absorption line could have been present outside of our velocity range.

All models considered thus far have explained an ESE as being due to an ionized object, either partially or totally ionized, occulting a background source. An alternate possibility is suggested by the decrease in the H I optical depth observed between the 1991 September 6 observations and the epochs during the ESE. If an ionizing source crossed the line of sight to 1741–038 and ionized some of the hydrogen, the result would be a decrease in the optical depth of the line. The difference in equivalent widths between 1991 September 6 and the epochs during the ESE is 1.47 km s^{-1} . The resulting total change in the column density, integrated over the line is $N_H = 2.7 \times 10^{19} \text{ cm}^{-2} (T_s/10 \text{ K})$.

We assume that any such ionized region would be comparable in extent to the angular diameter of 1741–038, about 0.5 mas (Fey, unpublished data). At a distance of 100 pc, the total quantity of hydrogen that would have been ionized was $1.2 \times 10^{43} (T_s/10 \text{ K}) (D/100 \text{ pc})^2$ atoms. An estimate of the ionizing rate required to maintain the ionization for this many atoms is, following Osterbrock (1989), at least $10^{38} \text{ s}^{-1} (T_s/10 \text{ K})^2 (D/100 \text{ pc})$, assuming that the ionized region was approximately spherical. An A0 star would suffice as an ionizing source.

4. Conclusions

We have determined the H I opacity spectra for 1741–038 at four epochs, including three as it underwent an extreme scattering event (Figure 2). The absorption spectra from the four epochs are dominated by a strong absorption feature centered on an LSR velocity of 5 km s^{-1} . The absorption feature itself is probably a blend of multiple components. Our absorption spectra are quite similar to a lower-resolution spectrum obtained by Dickey et al. (1983).

We find a secular trend of decreasing maximum optical depth during the decade between the observations of Dickey & Benson (1982), Dickey et al. (1983), and those reported here. In the early 1980s, $\tau \gtrsim 1$ toward 1741–038 while we find $\tau \simeq 0.7$.

We find no evidence for any change in the H I absorption feature during the ESE. Its equivalent width, maximum optical depth, and velocity at the maximum optical depth are all unchanged for the three epochs during the ESE. The maximum

optical depth change between any two epochs during the ESE is $\Delta\tau < 0.05$ (2.3σ) which we do not regard as significant.

The limit on the optical depth change, $\Delta\tau < 0.05$, implies a limit on the H I column density of any neutral structure(s) associated with the ESE lens, $N_H < 6.4 \times 10^{18} \text{ cm}^{-2} (T_s/100 \text{ K})$, having a spin temperature $T_s = 100 \text{ K}$. This limit poses no significant constraint on structures with $T_s \approx 200 \text{ K}$.

Some proposed colder structures are allowed. Tiny-scale atomic structures (Heiles 1997), with $T_s \approx 15 \text{ K}$ and $N_H \sim 3 \times 10^{18} \text{ cm}^{-2}$, are marginally ruled out, though geometric arguments may allow TSASs to be responsible for ESEs and meet this constraint on the H I column density. Walker & Wardle (1998) propose cold, H I-opaque molecular clouds in the Galactic halo. Any such structures within our observed velocity range are clearly excluded. However, the observed velocity range covers only 25% of the allowed range, so such a cloud could have been responsible for this ESE without violating our observational constraints.

We are grateful to E. Brinks for many helpful comments about the analysis of Galactic H I data. We are saddened that our thanks must be posthumous to the referee, R. Hjellming, for his comments that helped improve this paper. We also thank J. van Gorkom and S. Spangler for motivational comments. The National Radio Astronomy Observatory is a facility of the National Science Foundation operated under cooperative agreement by Associated Universities, Inc. Basic research in radio astronomy at the NRL is supported by the Office of Naval Research.

REFERENCES

- Clegg, A. W., Chernoff, D. F., & Cordes, J. M. 1988, in *Radio Wave Scattering in the Interstellar Medium*, eds. J. M. Cordes, B. J. Rickett, & D. C. Backer (New York: American Institute of Physics) p. 174
- Clegg, A. W., Fey, A. L., & Lazio, T. J. W. 1998, *ApJ*, 496, 253; astro-ph/9709249
- Cognard, I., Bourgois, G., Lestrade, J.-F., Biraud, F., Aubry, D., Darchy, B., & Drouhin, J.-P. 1993, *Nature*, 366, 320

- Dickey, J. M. & Benson, J. M. 1982, *AJ*, 87, 278
- Dickey, J. M., Kulkarni, S. R., Heiles, C. E., & van Gorkom, J. H. 1983, *ApJS*, 53, 59
- Fiedler, R., Dennison, B., Johnston, K. J., Waltman, E. B., & Simon, R. S. 1994, *ApJ*, 430, 581
- Fiedler, R. L., Dennison, B., Johnston, K. J., & Hewish, A. 1987a, *Nature*, 326, 675
- Fiedler, R. L., et al. 1987b, *ApJS*, 65, 319
- Frail, D. A., Weisberg, J. M., Cordes, J. M., & Mathers, C. 1994, 436, 144
- Goss, W. M., van Gorkom, J. H., & Shaver, P. A. 1979, *A&A*, 73, L17
- Heiles, C. 1997, *ApJ*, 481, 193
- Kulkarni, S. R. & Heiles, C. 1988, in *Galactic and Extragalactic Radio Astronomy*, eds. G. L. Verschuur & K. I. Kellermann (Springer-Verlag: Berlin) p. 95
- Lazio, T. J. W., et al. 2000a, *ApJS*, in preparation
- Lazio, T. J. W., et al. 2000b, *ApJ*, 534, 706; *astro-ph/9910323*
- Lestrade, J.-F., Rickett, B. J., & Cognard, I. 1998, *A&A*, 334, 1068
- Maitia, V., Lestrade, J.-F., & Cognard, I. 1998, *ApJ*, submitted
- Osterbrock, D. E. 1989, *Astrophysics of Gaseous Nebulae and Active Galactic Nuclei* (University Science Books: Mill Valley, CA)
- Phillips, J. A. & Wolszczan, A. 1991, *ApJ*, 382, L27
- Romani, R. W., Blandford, R. D., & Cordes, J. M. 1987, *Nature*, 328, 324
- Walker, M. & Wardle, M. 1998, *ApJ*, 498, L125; *astro-ph/9802111*
- Waltman, E. B., Fiedler, R. L., Johnston, K. J., Spencer, J. H., Florkowski, D. R., Josties, F. J., McCarthy, D. D., Matsakis, D. N. 1991, *ApJS*, 77, 379
- Wilcots, E. M., Brinks, E., & Higdon, J. 1997, *A Guide for VLA Spectral Line Observers*, Edition 9 (NRAO: Socorro, NM); <http://www.nrao.edu/vla/obstatus/splg1/>